The (Dimethylamino)methyl Radical. A Neutralization–Reionization and ab Initio Study

Scott A. Shaffer,† František Tureček,*,† and Ronald L. Cerny‡

Contribution from the Department of Chemistry, BG-10, University of Washington, Seattle, Washington 98195, and the Midwest Center for Mass Spectrometry, Department of Chemistry, University of Nebraska, Lincoln, Nebraska 68588-0362

Received July 2, 1993®

Abstract: The (dimethylamino)methyl radical (**1**) is generated in the gas phase by collisional neutralization of $(CH_3)_2N^+{=}CH_2$ ($\mathbf{1}^+$) with Xe, $(CH_3)_3N$, and CH_3SSCH_3 and by collisionally activated dissociation of ionized 1,2-bis(dimethylamino)ethane (**2**) at 8 keV and characterized by neutralization–reionization mass spectrometry. Vertical neutralization of $\mathbf{1}^+$ involves large Franck–Condon effects and produces **1** with ≥76 kJ mol^{-1} excess internal energy. Neutral **1** dissociates by loss of methyl to give $CH_3N{=}CH_2$ which undergoes further dissociation upon reionization. In contrast to vacuum pyrolysis, a significant fraction of **1** survives for 3.6 μs to yield 0.6–2.5% $\mathbf{1}^+$ after collisional reionization with O_2, ICl, NO_2, and $TiCl_4$, whereas >25% of **1** survives after collisionally activated dissociation of $\mathbf{2}^{\bullet+}$. Equilibrium geometries of **1** and $\mathbf{1}^+$ from ab initio calculations with the 6-31G* basis set substantially differ in the C–N bond lengths and pyramidization at N and CH_2. Calculations using the Møller–Plesset theory at the MP4(SDTQ)/6-31G* and MP4(SDQ)/6-311G** levels with zero-point vibrational energy corrections are used to estimate the relative stabilities of **1**, $\mathbf{1}^+$, and their ionic and neutral dissociation products. The vertical ionization energies of **1** and C_2H_5N isomers are calculated and evaluated at the MP2 and MP4/6-311G** levels of theory. Large Franck–Condon effects are predicted by theory and found by experiment in the vertical neutralization of $CH_3N{=}CH_2^{\bullet+}$ and aziridine$^{\bullet+}$. Stable $^{\bullet}H_2CNHCH_2^{\bullet}$ biradical is prepared by neutralization of $^+CH_2NHCH_2^{\bullet}$ and predicted to be the ($^1A_1$) singlet electronic state.

α-Aminoalkyl radicals are electron-rich transient species whose ionization energies (IE)[1] and half-wave potentials[2] approach those of alkali metals.[3] Oxidation of α-aminoalkyl radicals yields very stable immonium cations that also appear as intermediates in the Mannich[4] and Polonovski reactions,[5] and whose gas-phase chemistry has been studied extensively by mass spectrometry.[6] The (dimethylamino)methyl radical, $(CH_3)_2NCH_2^{\bullet}$ (**1**), is formed, *inter alia*, in aqueous solution by the reaction of trimethylamine with hydroxyl or alkoxyl radicals produced by photolysis[7] or pulse radiolysis.[8] In a gas-phase study, Lossing and co-workers cogenerated radical **1** and its cation, $(CH_3)_2NCH_2^+$ ($\mathbf{1}^+$), by dissociative ionization of 1,2-bis(dimethylamino)ethane (**2**) and determined their heats of formation (ΔH_f) from thermochemical cycles based on appearance energy measurements.[1] The adiabatic ionization energy of **1**, estimated as 5.35–5.7 eV from $\Delta H_f(\mathbf{1}^+) - \Delta H_f(\mathbf{1})$,[1,9] is close to that of sodium (5.13 eV), justifying the description of **1** as an "organic metal".[1b] Although the chemistry of **1** in solution has been studied in considerable detail by experiment[4,5,7,8a,b] and theory,[10] the dissociations and electron transfer reactions of gaseous **1** have been unknown. An attempt at generating **1** in the gas phase by pyrolysis of 1,2-bis(dimethylamino)ethane (**2**) yielded *N*-methylmethylenimine, a presumed product of thermal decomposition of **1**.[11]

In this paper we report on the preparation of **1** by collisional neutralization of ion $\mathbf{1}^+$ with gaseous targets of different ionization energies. According to previous studies of gas-phase electron transfer[12] this could presumably result in the formation of **1** with different excitation energies, depending on the difference between the vertical recombination energy of $\mathbf{1}^+$ and the target vertical ionization energy.[12] Due to the very low estimated ionization energy of **1**, and hence a low recombination energy of ion $\mathbf{1}^+$, collisional neutralization of the latter by electron transfer from closed-shell organic molecules is practically always endothermic.[3] We also address the question of ion stability following reionization of **1** with gaseous targets of increasing electron affinity. The exceptionally low ionization energy of **1** allows one to study electron capture near the thermoneutrality level. **1** thus represents a convenient model for studying both the neutralization and reionization phenomena. Although the internal energy of both **1** produced by neutralization and $\mathbf{1}^+$ following reionization is not measured, it can be followed indirectly through competitive unimolecular dissociations of **1** and $\mathbf{1}^+$ using neutralization–

† University of Washington.
‡ University of Nebraska.
® Abstract published in *Advance ACS Abstracts,* December 1, 1993.

(1) (a) Griller, D.; Lossing, F. P. *J. Am. Chem. Soc.* **1981**, *103*, 1586–1587. (b) Burkey, T. J.; Castelhano, A. L.; Griller, D.; Lossing, F. P. *J. Am. Chem. Soc.* **1983**, *105*, 4701–4703.
(2) (a) Wayner, D. D. M.; McPhee, D. J.; Griller, D. *J. Am. Chem. Soc.* **1988**, *110*, 132–137. (b) Wayner, D. D. M.; Dannenberg, J. J.; Griller, D. *Chem. Phys. Lett.* **1986**, *131*, 189–191.
(3) Lias, S. G.; Bartmess, J. E.; Liebman, J. F.; Holmes, J. L.; Levin, R. D.; Mallard, W. G. *J. Phys. Chem. Ref. Data, Suppl. 1* **1988**, *17*, 95.
(4) Böhme, H.; Viehe, H. G., Eds. *Imminium Salts in Organic Chemistry*; Wiley: New York, 1976; Part 1.
(5) Manninen, K.; Hakala, E. *Acta Chem. Scand. Ser. B* **1986**, *B40*, 598–600.
(6) (a) Ucella, N. A.; Howe, I.; Williams, D. H. *J. Chem. Soc. B* **1971**, 1933. (b) Cum, G.; Romeo, G.; Ucella, N. *Org. Mass Spectrom.* **1974**, *9*, 365–371. (c) Levsen, K.; McLafferty, F. W. *J. Am. Chem. Soc.* **1974**, *96*, 139–144. (d) Veith, H. J.; Gross, J. H. *Org. Mass Spectrom.* **1991**, *26*, 1061–1064. (e) Veith, H. J.; Gross, J. H. *Org. Mass Spectrom.* **1991**, *26*, 1097–1108. (f) Wlodek, S.; Bohme, D. K. *J. Am. Chem. Soc.* **1988**, *110*, 2396–2399. (g) For a review see: Bowen, R. D. *Mass Spectrom. Rev.* **1991**, *10*, 225–279.
(7) MacInnes, I.; Walton, J. C.; Nonhebel, D. C. *J. Chem. Soc., Perkin Trans. 2* **1987**, 1789–1793.
(8) (a) Das, S.; von Sonntag, C. *Z. Naturforsch.* **1986**, *41b*, 505–513. (b) Das, S.; Schuchmann, N.; Schuchmann, H.-P.; von Sonntag, C. *Chem. Ber.* **1987**, *120*, 319–323. For radiolytic formation of **1** by ion–molecule reactions see: (c) Helner, L.; Sick, L. W. *Int. J. Chem. Kinet.* **1973**, *5*, 177. (d) Brupbacher, J. M.; Eagle, G. J. *J. Phys. Chem.* **1975**, *79*, 671. (e) Belevsky, V. N.; Belopushkin, S. I.; Feldman, V. I. *J. Radioanal. Nucl. Chem. Lett.* **1986**, *107*, 81–93.
(9) Loguinov, Y.; Takhistov, V. V.; Vatlina, L. P. *Org. Mass Spectrom.* **1981**, *16*, 239–241.
(10) Armstrong, D. A.; Rauk, A.; Yu, D. *J. Am. Chem. Soc.* **1993**, *115*, 666–673.
(11) Werstiuk, N. H. *Can. J. Chem.* **1986**, *64*, 2175–2183.
(12) Holmes, J. L. *Mass Spectrom. Rev.* **1989**, *8*, 513–539.

0002-7863/93/1515-12117$04.00/0

reionization (NR) mass spectrometry[13] combined with collisional activation of the intermediate radicals.[14] The recombination and ionization energies are further assessed with the help of ab initio calculations.

Experimental Section

Measurements were carried out with a tandem quadrupole acceleration–deceleration mass spectrometer designed for neutralization–reionization studies.[14] Precursor ions of approximately 80 eV kinetic energy were generated by electron ionization (electron energy 70 eV, emission current 400 μA, ion source temperature 130 °C), passed through a quadrupole mass filter operated in the radio frequency only mode,[15] and accelerated to 8250 eV. Neutralization of fast ions with xenon (Airco, 99.95%), trimethylamine (Matheson, 99.0%), and dimethyl disulfide (Aldrich, 99%) was carried out such as to achieve 70% ion beam transmittance (T) in a differentially pumped collision cell floated at −8170 V. The mixture of ions and neutrals enters a cylindrical conduit floated at +210 V which allows passage of neutral species while rejecting the ions. After travelling 60 cm (3.6 μs for a neutral of mass 58 Da) the neutrals are reionized to cations in a differentially pumped collision cell floated at a variable high voltage defining the potential energy of the ions formed. Oxygen, iodine monochloride (Aldrich, 98%), nitrogen dioxide (Matheson, 99.5%), and titanium tetrachloride (Aldrich, 99.9%) were admitted in the reionization cell at a pressure such as to achieve 70% precursor ion beam transmittance. The cations were decelerated by an electrostatic lens, energy-filtered, and mass-analyzed by a quadrupole filter as MS-II which was scanned in link with the deceleration voltage.[14]

These linked scans achieve both precursor and product ion resolution even without prior precursor ion separation, owing to the unique combination of the m/z and kinetic energy for each product ion. The precursor ion mass resolution is given by $m/\Delta m = e|U_{dec}|/\Delta E$, where m is the mass of the precursor ion, U_{dec} is the deceleration voltage, and ΔE is the band width of the energy-filter lens (ca. 25 eV).[14] This corresponds to precursor mass resolution of $m/\Delta m$ = 85–330 for product ions of m/z 15–58, formed from a precursor of m/z 58. Precursors at adjacent m/z values were thus resolved throughout the NR spectrum. The product ion mass resolution is determined by the quadrupole filter parameters that were set to achieve 0.4 u peak width (full width at half maximum) to ensure unit mass resolution (10% valley) in most measurements. Typically, 15–30 repetitive scans were taken using a PC-based data acquisition system[16] to achieve base peak signal-to-noise ratios >500.

Collisionally activated dissociation (CAD) at kiloelectronvolt kinetic energy of the radicals formed by neutralization was carried out by admitting helium to the differentially pumped conduit between the neutralization and reionization cells to achieve 50% transmittance of the precursor ion beam. Any ions formed by collisional reionization with He in the conduit pass the deceleration lens with high kinetic energies (<8460 eV) and are stopped by the energy filter,[14] so that only products of neutral CAD are detected.

CAD of 8 keV ions using O_2 at 70% beam transmittance was carried out in the third field-free region of a Kratos MS-50T spectrometer.[17] The precursor ion was selected by the electric (E) and magnet (B) sectors, and the CAD spectrum was obtained as a kinetic energy scan. CAD of the deuterium labeled derivatives (4 keV, O_2, 70% transmittance) was carried out on a Kratos Profile double-focusing mass spectrometer of a forward (E precedes B) geometry furnished with a home-built collision cell mounted in the first field-free region. The spectra were obtained by scanning the E and B sectors while keeping the B/E ratio constant. The product ion mass resolution in these scans was >300. The CAD spectra were averaged over 6 repetitive scans in which the fragment relative intensities varied by <3%.

1,2-Bis(dimethylamino)ethane (**2**) and 1,4-bis(dimethylamino)butane (**3**) (Aldrich) were distilled in vacuo before use. 1,4-Bis(dimethylamino)-butane-*1,1,4,4-d*$_4$ (**4**) was prepared by lithium aluminum deuteride (Aldrich, 98% *d*) reduction of *N,N,N',N'*-tetramethylsuccinamide in tetrahydrofuran and distilled in vacuo, bp 68–70 °C (20 Torr). *N,N*-(Dimethylamino)heptane (**5**) and (methyl-d_3-methylamino)heptane (**6**) were prepared by standard methods as shown in Scheme I. Derivatives **4–6** gave satisfactory 200 MHz ^{1}H-NMR and mass spectra. Aziridine was prepared by a standard procedure.[18]

Scheme I

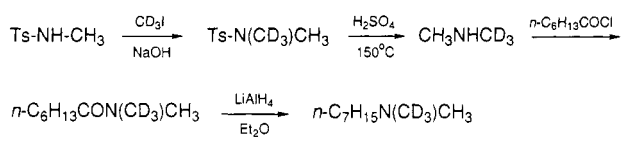

Calculations

Standard ab initio molecular orbital calculations were carried out using the GAUSSIAN 92 suite of programs.[19] Geometries were first optimized with the 3-21G basis set and then reoptimized with the 6-31G* basis set. Spin-unrestricted (UHF) wave functions were used for open-shell species. 6-31G* and 3-21G (for **1** and **1**$^+$) harmonic vibrational frequencies were used to characterize stationary points as potential energy minima (all frequencies real) and (after scaling by 0.9) to calculate zero-point vibrational contributions to relative energies. The optimized geometries and harmonic frequencies are available as Supplementary Material. Improved relative energies were obtained through calculations on the HF/6-31* optimized geometries using the Møller–Plesset perturbation theory (frozen core) terminated at fourth (MP4) order. The MP4(SDTQ)/6-31* electronic energies corrected for zero-point vibrational energies were used to calculate relative energies at 0 K. The harmonic vibrational frequencies were used to calculate molar enthalpies at 298 K using the rigid-rotor-harmonic-oscillator approximation; the 298 K relative energies are discussed in the text. MP4(SDTQ) calculations with the larger 6-311G** basis set using the optimized 6-31G* geometries were also employed to estimate ionization and recombination energies of the C_2H_5N isomers. For **1** and **1**$^+$ MP4 calculations including triplet excitations became too time consuming and the latter were omitted. These relative energies therefore refer to MP4(SDQ)/6-311G**//6-31G*.

Results and Discussion

Preparation of transient gaseous species by collisional neutralization relies upon the knowledge of the precursor ion structure and chemistry. The dissociations of the *N,N*-dimethylmethyleniminium ion (**1**$^+$), as elucidated by deuterium labeling, are therefore discussed briefly.

Ion Dissociations. Ion **1**$^+$, which served as a precursor for radical **1**, is a well-characterized species formed by α-cleavage dissociative ionization of a variety of precursors of the R-CH_2N-$(CH_3)_2$ type.[6g] In this work we have used dissociative ionization of amines **3** and **5** to prepare **1**$^+$. Ionized amines **3** and **5** have comparable total numbers of atoms ($C_8H_{20}N_2$ and $C_9H_{19}N$, respectively), and hence comparable numbers of vibrational degrees of freedom, to form ions **1**$^+$ of comparable internal energies. Deuterium-labeled precursors **4** and **6** were used to generate $(CH_3)_2N^+{=}CD_2$ (**1a**$^+$) and $(CD_3)(CH_3)N^+{=}CH_2$ (**1b**$^+$), respectively. In the 70-eV electron impact mass spectra of all these precursors the corresponding **1**$^+$ ions represent the predominating base peaks (>50% of total ion current) free of isotopic and isobaric interferences as corroborated by the clean mass shifts of m/z 58 to 60 and 61, for **4** and **6**, respectively. The CAD spectra of **1**$^+$ measured for ions of 8 and 4 keV kinetic

(13) (a) Danis, P. O.; Wesdemiotis, C.; McLafferty, F. W. *J. Am. Chem. Soc.* **1983**, *105*, 7454–7456. (b) Burgers, P. C.; Holmes, J. L.; Mommers, A. A.; Terlouw, J. K. *Chem. Phys. Lett.* **1983**, *102*, 1–3. For a recent review see McLafferty, F. W. *Science (Washington, D.C.)* **1990**, *247*, 925–929.

(14) Turecek, F.; Gu, M.; Shaffer, S. A. *J. Am. Soc. Mass Spectrom.* **1992**, *3*, 493–501.

(15) Dawson, P. *Mass Spectrom. Rev.* **1986**, *5*, 1–37.

(16) Drinkwater, D. E.; Turecek, F.; McLafferty, F. W. *Org. Mass Spectrom.* **1991**, *26*, 559–562.

(17) Gross, M. L.; Chess, E. K.; Lyon, P. A.; Crow, F. W. *Int. J. Mass Spectrom. Ion Phys.* **1982**, *42*, 243–254.

(18) Allen, C. F. H.; Spangler, F. W.; Webster, E. R. *Org. Synth.* **1950**, *30*, 38–40.

(19) Gaussian 92, Revision C.; Frisch, M. J.; Trucks, G. W.; Head-Gordon, M.; Gill, P. M. W.; Wong, M. W.; Foresman, J. B.; Johnson, B. G.; Schlegel, H. B.; Robb, M. A.; Replogle, E. S.; Gomperts, R.; Andres, J. L.; Raghavachari, K.; Binkley, J. S.; Gonzalez, C.; Martin, R. L.; Fox, D. J.; DeFrees, D. J.; Baker, J.; Stewart, J. J. P.; Pople, J. A.; Gaussian Inc.: Pittsburgh, PA, 1992.

Table I. CAD (O_2, 50% transmittance, *T*), NR (CH_3SSCH_3, 70% T/O_2, 70% *T*), and NCR (CH_3SSCH_3, 70% *T*/He, 50% T/O_2, 70% *T*) Mass Spectra of $\mathbf{1}^+$, $\mathbf{1a}^+$, and $\mathbf{1b}^+$

	$(CH_3)_2N^+{=}CH_2$			$(CH_3)_2N^+{=}CD_2$			$CH_3(CD_3)N^+{=}CH_2$		
m/z	CAD[b]	NR	NCR	CAD	NR	NCR	CAD	NR	NCR
61								5.4	2.6
60					2.7	0.8	6.4	0.2	0.2
59				7.0	0.2		4.1		0.2
58		3.7	2.2	4.8			2.5		
57	10.1	0.4	0.4	2.6			0.6		
56	3.5			0.8	0.1		0.9	0.15	0.4
55	0.7			0.4			0.3		
54	1.4		0.1						
47							0.3		
46							3.3	1.3	0.9
45				5.9	2.0	1.5	13.9	9.8	8.6
44				17.7	5.6	4.4	8.5	2.5	1.4
43	6.6	2.4	1.6	16.1	15.4	11.2	6.5	3.6	3.6
42	40.3	19.4	16.8	6.6	6.5	5.4	20.8	12.1	9.6
41	9.6	7.8	7.3	2.7	3.7	4.0	5.2	4.5	3.8
40	4.5	6.8	6.6	1.3	3.3	2.8	2.7	4.1	3.7
39	1.2	3.2	3.3	0.4	1.7	1.4	0.8	1.25	1.6
38	0.7	2.7	2.9	0.3	1.8	2.1	0.6	2.6	1.9
33							3.0	0.1	0.1
32	0.2			4.7		0.2	4.8	0.2	0.25
31				12.2	0.2	0.2	5.9	0.5	0.3
30	11.6	0.4	0.5	10.7	5.0	5.3	3.7	2.4	2.7
29	3.4	0.55	0.25	2.4	4.2	3.5	2.5	1.9	2.0
28	3.9	9.9	10.9	2.2	11.2	14.4	2.3	9.5	9.8
27	2.0	14.1	15.7	0.9	8.0	11.3	0.5	12.1	13.2
26	0.3	8.5	8.9	0.3	7.3	8.6		5.7	8.7
25		1.1	2.4		0.6	0.8		0.8	0.6
24		0.4	1.0		0.4	1.1		0.3	0.5
18								6.0	8.4
17					1.8	1.1		0.9	0.5
16		0.2	0.05		2.2	2.4		3.3	3.6
15		8.5	8.5		6.6	8.8		3.2	3.8
14		6.1	6.1		6.0	4.5		3.1	4.6
13		2.5	2.8		1.8	2.2		1.2	1.3
12		1.4	1.7		1.8	2.0		1.0	1.3

[a] Percent relative to the sum of ion intensities (integrated peak areas). [b] Ions at $m/z < 26$ were not recorded in these CAD spectra obtained by B/E linked scans.

energy are similar to that reported previously[6c] and show the dominant elimination of methane (forming $C_2H_4N^+$ at *m/z* 42), in addition to losses of a hydrogen atom (*m/z* 57) and methyl (*m/z* 43) and formation of $CH_2{=}NH_2^+$ (*m/z* 30, Table I). Deuterium labeling in one methyl group ($\mathbf{1b}^+$) showed a preferential loss of CH_4, $[M - CH_4]^+/[M - CH_3D]^+ = 1.77$,[20] whereas $\mathbf{1a}^+$ showed $[M - CH_4]^+/[M - CH_3D]^+ = 1.22$. This allows one to calculate both the branching ratio, $k_1/k_2 = 1.2$ for the methane elimination involving hydrogen atom transfer from the methylene (k_1) and methyl (k_2) groups, and an intramolecular deuterium isotope effect, $k_H/k_D = 1.47$ for the methane eliminations. The preferential hydrogen transfer from the methylene group in $\mathbf{1}^+$ is consistent with the greater stability of the $CH_3N^+{\equiv}CH$ ion formed,[21] compared with that of $CH_2{=}N^+{=}CH_2$ formed by the competing elimination (Scheme II), as discussed below.

Neutral Formation. Collisional neutralization of $\mathbf{1}^+$ followed by reionization of **1** results in the formation of stable survivor ions (Figure 1, Table I). This shows that the intermediate radical **1** is stable for >3 μs under collision-free conditions in contrast to its complete dissociation under pyrolytic conditions.[11] The relative abundance of reionized $\mathbf{1}^+$ depends on the nature of both the neutralization and reionization gases. We find dimethyl disulfide as a mild neutralization reagent yielding the highest abundance of surviving $\mathbf{1}^+$ (3.7% of the sum of NR peak intensities, Figure 1) following reionization with oxygen. Xenon or trimethylamine lead to less abundant reionized $\mathbf{1}^+$ (0.6 and 0.7%, respectively, Table II). These data suggest that, contrary to previous reports,[12,22] there is no clear-cut relationship between the neutralization endothermicity (ΔE_n = ion recombination energy – target vertical ionization energy) and the stability of the incipient **1**. For xenon (IE_v = 12.13 eV), dimethyl disulfide (IE_v = 8.97 eV),[23] and trimethylamine (IE_v = 8.45 eV),[23] the neutralization is endothermic by 7.6, 4.5, and 4 eV, respectively, based on the calculated recombination energy (RE) of $\mathbf{1}^+$ (4.5 eV, vide infra).

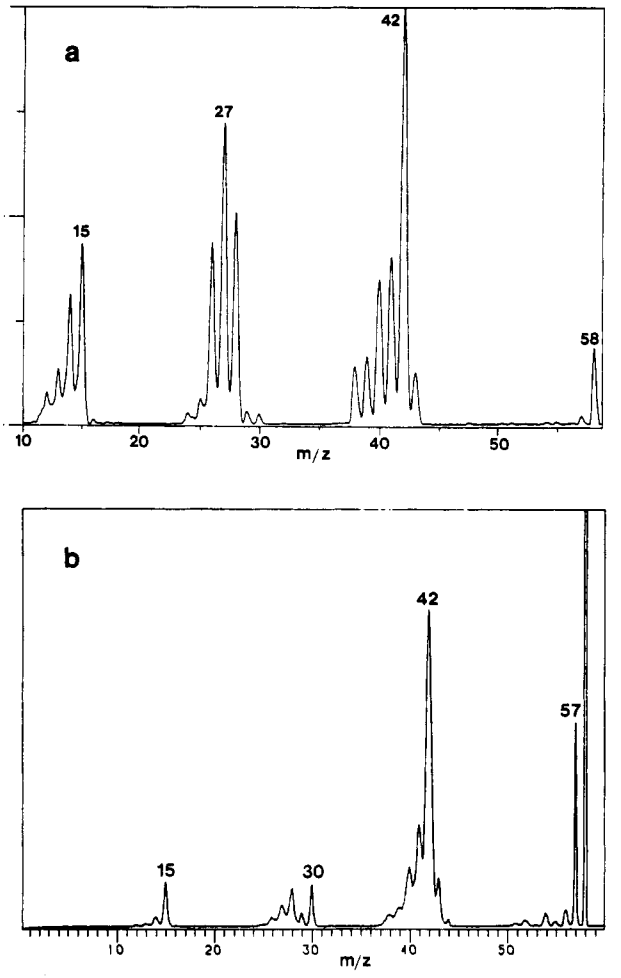

Figure 1. (a) Neutralization–reionization (CH_3SSCH_3/O_2, 70% transmittance) and (b) CAD (O_2, 70% transmittance) spectra of $\mathbf{1}^+$.

Scheme II

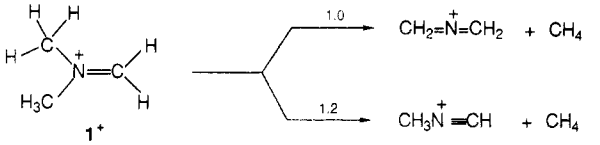

(20) The relative intensities of $(M - CH_3D)^+$ ions were corrected for the contributions from the isobaric $(M - CH_4 - H)^{•+}$ ions by using the relative intensities of the corresponding ions in the CAD or NR mass spectra of $\mathbf{1}^+$ and the statistical weights for H or D losses.

(21) (a) Wurthwein, E.-U. *J. Org. Chem.* **1984**, *49*, 2971–2978. (b) Nguyen, M. T.; Ha, T.-K. *J. Chem. Soc., Perkin Trans. 2* **1984**, 1401–1405. (c) Malone, S.; Hegarty, A. F.; Nguyen, M. T. *J. Chem. Soc., Perkin Trans. 2*, **1988**, 477–483.

(22) (a) Hop, C. E. C. A.; Holmes, J. L. *Org. Mass Spectrom.* **1991**, *26*, 476–480. (b) Beranova, S.; Polce, M. J.; Boyle, S. V.; Wesdemiotis, C. *Proceedings of the 40th ASMS Conference on Mass Spectrometry and Allied Topics*, Washington, DC, 1992, Comm. No. WP 177. (c) Smith, R. W.; Suh, D.; Burgers, P. C.; Terlouw, J. K. *Proceedings of the 40th ASMS Conference on Mass Spectrometry and Allied Topics*, Washington, DC, 1992, Comm. No. TP 120.

(23) (a) Levin, R. D.; Lias, S. G. *Ionization and Appearance Potential Measurements 1971–1981*; NSRDS, National Bureau of Standards; U.S. Government Printing Office: Washington, DC, 1982. (b) Kimura, K.; Katsumata, S.; Achiba, Y.; Yamazaki, T.; Iwata, S. *Handbook of He(I) Photoelectron Spectra of Fundamental Organic Molecules*; Japan Scientific Societies Press: Tokyo, 1981.

Table II. Neutralization–Reionization Spectra of $(CH_3)_2N^+{=}CH_2$

	relative intensity[a,b]					
m/z	Xe/O_2	Xe/ICl	Xe/NO_2	Xe/$TiCl_4$	$(CH_3)_3$-N/O_2	He-(CAD)/O_2
58	0.6	2.5	1.8	1.5	0.7	25.4
57	0.2			0.1		5.8
56						0.8
55	0.1					
54	0.2			0.1		
44						0.9
43	1.4	1.1	1.3	0.9	0.6	4.1
42	15	22	18	18	9.2	25.4
41	7.6	8.0	8.6	6.5	4.0	10.3
40	6.1	6.8	7.6	6.3	3.5	4.7
39	3.0	1.7	2.6	3.3	2.1	1.6
38	2.7	1.6	2.6	2.0	1.7	0.8
30	0.3		0.2	0.1	0.1	2.5
29	0.8	0.6	0.4	0.6	0.5	1.3
28	16	14	15	15	14	6.8
27	18	16	22	12	17	6.5
26	11	5.3	6.9	5.6	11	2.8
25	1.5	0.9	0.6	0.6	1.7	0.5
24	0.3		0.2	0.1	0.8	
16		0.2			0.5	
15	8.6	14	6.6	24	20	
14	4.3	3.2	3.9	7.4	19	
13	1.7	1.3	1.2	2.6	1.9	
12	0.9	0.9	0.7	1.6	0.4	

[a] Percent relative to the sum of reionized peak intensities. [b] NR efficiencies (ΣNR/[precursor], ref 27d) were as follows: Xe/O_2 1.0×10^{-4}, Xe/ICl 7.3×10^{-6}, Xe/NO_2 1.6×10^{-5}, Xe/$TiCl_4$ 0.001.

Significant effects on the survivor ion stability are also observed in reionization of Xe-formed **1** with targets of increasing electron affinity (EA), e.g., ICl (EA = 1.5–2.4 eV),[3] NO_2 (EA = 2.3 eV),[3] and $TiCl_4$ (EA = 2.9 eV)[3]. There is no direct correlation between the reionization endothermicity (defined as ΔE_r = EA(target) – IE_v(**1**)) and the relative intensity of the surviving $\mathbf{1}^+$, with ICl ($\Delta E_r > 3.8$ eV) giving the highest [$\mathbf{1}^+$] whereas O_2 (ΔE_r = 5.8 eV), NO_2 (ΔE_r = 3.9 eV), and $TiCl_4$ (ΔE_r = 3.3 eV) cause more dissociation (Table II). The sensitivity of [$\mathbf{1}^+$] toward the neutralization and reionization conditions suggests that both neutral and ion dissociations are taking place following electron transfer.

Note also that there is no smooth relationship between the reionization *efficiency* of **1** and the target EA, although reionization of **1** with the target of highest EA ($TiCl_4$) is ten times more efficient than reionization with O_2 (Table II). Unfortunately, $TiCl_4$ was found to have a devastating effect on the electron multiplier used for NRMS ion detection, so we were forced to discontinue the use of $TiCl_4$ as reionization reagent in spite of its high efficiency.

In contrast to the NR spectra, a very abundant survivor peak of $\mathbf{1}^+$ (~25%Σ[NR]) is obtained by O_2 reionization of the *neutral* fragment **1** formed by CAD(He) of ion $\mathbf{2}^{\bullet+}$ at 8 keV kinetic energy (Table II). The CAD spectrum of $\mathbf{2}^{\bullet+}$ shows predominant formation of $\mathbf{1}^+$ (84% of total CAD ion current), suggesting an efficient formation of the complementary radical **1**. The CAD/reionization (also termed neutral-fragment reionization)[24] spectrum of $\mathbf{2}^{\bullet+}$ indicates that **1** is very stable if formed by ion dissociation in spite of the hard collision gas used.[25] CAD and collisional electron transfer can differ in the amount of internal energy imparted in the incipient neutral.[26] In CAD the precursor ion is excited in $<10^{-14}$ s, but its dissociations take place within microseconds, thus allowing the internal energy to be distributed among the internal degrees of freedom of the ionic and neutral

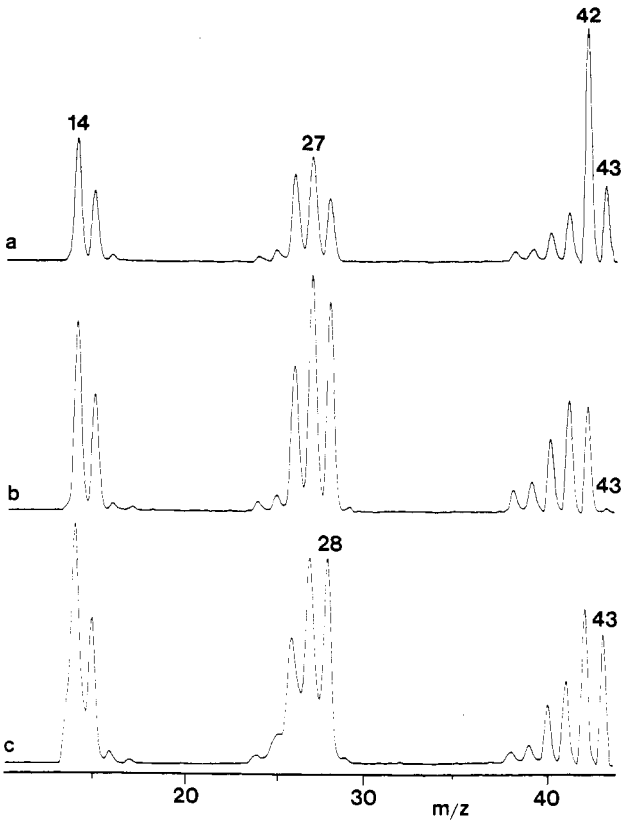

Figure 2. NR(CH_3SSCH_3/O_2, 70% *T*) mass spectra of (a) CH_3-N=$CH_2^{\bullet+}$, (b) aziridine$^{\bullet+}$, and (c) $^{\bullet}CH_2NHCH_2^+$.

part. For a <2 eV average energy deposition upon CAD[25] and the 0.6–0.7 eV bond dissociation energy in $\mathbf{2}^{\bullet+}$,[1,9] a large fraction of **1** is formed with <0.5(2 – 0.65) = 0.67 eV internal energy, i.e. below the dissociation threshold. By contrast, vertical neutralization can lead to internal excitation through unfavorable Franck–Condon factors,[26] as discussed below.

The NR mass spectrum of **1** shows abundant fragments at *m/z* 38–43 due to losses of (C,H_x), *m/z* 26–28 (CN^+, $HCN^{\bullet+}$, H_2CN^+), and *m/z* 12–15 (CH_x^+), whereas the loss of H, typical for CAD of $\mathbf{1}^+$, is negligible. Although the relative intensities of the ions within the *m/z* 38–43 group are similar in the NR and CAD spectra of $\mathbf{1}^+$, deuterium labeling reveals different dissociation mechanisms (Table I). Evaluation of the [M – C(H,D)$_4$] intensities in the NR spectra[20] shows high preference for the loss of the methylene hydrogen together with one of the methyl groups. After correction for the calculated intramolecular deuterium isotope effect, $k_H/k_D = 1.62$, the branching ratio for the loss of methyl with the methylene and methyl hydrogens is 3.88. The secondary isotope effect in the loss of (CH_3 + H,D) and (CD_3 + H) from **1b** is relatively small, [M – (CH_3 + H,D)]$^+$/[M – (CD_3 + H)]$^+$ = 1.24.

Although the presence of the $C_2H_4N^+$ fragment formally points to elimination of CH_4 from **1**, the peaks of $CH_4^{\bullet+}$ and $CD_3H^{\bullet+}$ due to reionization of neutral methane are negligibly small in the NR spectra of **1** and **1b**, which nevertheless contain abundant CH_3^+ and CD_3^+ ions, respectively (Table I). By comparison, methane is found to give a significant survivor ion,[27] e.g., following exothermic neutralization with CH_3SSCH_3 (ΔE = 3.6 eV) and reionization with O_2, $[CH_4]^{\bullet+}/[CH_3]^+ = 0.11$, so that formation of CH_4 from **1** would have been detected. The absence of the

(24) Cordero, M. M.; Houser, J. J.; Wesdemiotis, C. *Anal. Chem.* **1993**, *65*, 1594–1601.
(25) Kim, M. S. *Org. Mass Spectrom.* **1991**, *26*, 565–574.
(26) (a) van Baar, B. L. M.; Burgers, P. C.; Holmes, J. L.; Terlouw, J. K. *Org. Mass Spectrom.* **1988**, *23*, 355–363. (b) Hop, C. E. C. A.; Holmes, J. L. *Int. J. Mass Spectrom. Ion Processes* **1991**, *104*, 213–226.
(27) (a) Zhang, M.-Y.; McLafferty, F. W. *J. Am. Soc. Mass Spectrom.* **1992**, *3*, 108–112. (b) Hop, C. E. C. A.; Holmes, J. L.; Wang, M. W.; Radom, L. *Chem. Phys. Lett.* **1989**, *159*, 580–586. (c) Bordas-Nagy, J.; Holmes, J. L.; Hop, C. E. C. A. *Int. J. Mass Spectrom. Ion Processes* **1988**, *85*, 241–258. (d) Wesdemiotis, C.; Feng, R.; Williams, E. R.; McLafferty, F. W. *Org. Mass Spectrom.* **1986**, *21*, 689–695.

Table III. Total Energies of Neutral and Ionic Species Calculated with the 6-31G* Basis Set

species	symmetry	total energy[a] HF	MP2	MP4(SDTQ)	ZPVE[b]	ΔH_{298}[c]
1	C_s	−172.644 976	−173.180 530	−173.243 650	269.0	18.0
1 (I)[e]	C_{2v}	−172.618 696	−173.154 427	−173.216 612		
$\mathbf{1}^+$	C_{2v}	−172.468 001	−173.006 216	−173.069 009	280.7	16.5
$\mathbf{1}^+$ (N)[d]	C_s	−172.416 268	−172.966 676	−173.031 920		
$CH_3N{=}CH_2$	C_s	−133.061 490	−133.476 976	−133.522 253	174.1	12.8
$CH_3N{=}CH_2$ (I)	C_s	−133.022 393	−133.437 055	−133.482 241		
$CH_3N{=}CH_2^{•+}$	C_s	−132.780 031	−133.145 970	−133.197 562	166.8	14.7
$CH_3N{=}CH_2^{•+}$ (N)	C_s	−132.754 582	−133.120 113	−133.171 990		
aziridine	C_s	−133.038 559	−133.458 987	−133.500 858	179.5	11.0
aziridine (I)	C_s	−133.008 964	−133.429 604	−133.471 279		
aziridine$^{•+}$	C_s	−132.750 431	−133.128 206	−133.175 394	172.4	12.0
aziridine$^{•+}$ (N)	C_s	−132.726 677	−133.109 574	−133.156 403		
$\mathbf{7}^{•+}$ ($^2A_2$)	C_{2v}	−132.807 667	−133.176 914	−133.224 976	171.7	12.6
7 ($^1A_1$)	C_{2v}	−132.977 049	−133.414 999	−133.458 378	171.9	13.2
7 (I)	C_{2v}	−132.974 226	−133.415 040	−133.458 954		
8	C_1	−132.986 367	−133.363 162	−133.408 890	162.2	14.9
8 (I)	C_{2v}	−132.969 137	−133.345 045	−133.389 765		
$CH_2{=}NCH_2^•$	C_{2v}	−132.457 108	−132.827 373	−132.875 286	135.2	12.5
$CH_2{=}N^+{=}CH_2$	D_{2d}	−132.214 382	−132.607 455	−132.651 147	145.7	12.5
(*Z*)-$CH_3N{=}CH^•$	C_s	−132.425 604	−132.809 617	−132.856 081	138.1	13.0
$CH_3N^+{\equiv}CH$	C_{3v}	−132.221 987	−132.621 312	−132.660 661	145.1	12.7
$CH_2CH_2N^•$	C_{2v}	−132.429 850	−132.815 698	−132.860 848	142.9	11.0
CH_4	T_d	−40.195 172	−40.332 442	−40.354 544	112.9	10.0
$CH_3^•$	C_{3v}	−39.558 992	−39.668 669	−39.689 177	73.2	11.1
$H^•$		−0.498 233				6.2

[a] In hartrees, 1 hartree = 2625.5 kJ mol^{-1} = 27.2115 eV. [b] Zero-point vibrational energies (kJ mol^{-1}) calculated from 6-31G* harmonic frequencies scaled by 0.9. [c] 298 K enthalpy corrections (kJ mol^{-1}) calculated using the rigid-rotor-harmonic oscillator approximation. [d] N: single-point calculations of ions on optimized neutral geometries. [e] I: single-point calculations of neutral species on optimized ion geometries.

Table IV. Total Energies of Neutral and Ionic Species Calculated with the 6-311G** Basis Set

species	total energy[a] HF	MP2	MP4(SDQ)	MP4(SDTQ)
1	−172.691 760	−173.307 078	−173.357 527	
1 (I)[b]	−172.667 251	−173.282 673	−173.332 356	
$\mathbf{1}^+$	−172.512 955	−173.121 763	−173.169 882	
$\mathbf{1}^+$ (N)[c]	−172.460 975	−173.082 356	−173.129 698	
$CH_3N{=}CH_2$	−133.096 369	−133.563 532	−133.595 928	−133.614 093
$CH_3N{=}CH_2$ (I)	−133.059 957	−133.525 471	−133.558 118	−133.576 063
$CH_3N{=}CH_2^{•+}$	−132.814 243	−133.223 828	−133.265 888	−133.279 971
$CH_3N{=}CH_2^{•+}$ (N)	−132.785 262	−133.196 586	−133.238 399	−133.252 621
aziridine	−133.075 081	−133.548 258	−133.577 743	−133.595 420
aziridine (I)	−133.045 793	−133.519 111	−133.548 561	−133.566 112
aziridine$^{•+}$	−132.785 619	−133.208 125	−133.245 308	−133.259 830
aziridine$^{•+}$ (N)	−132.762 541	−133.190 452	−133.226 666	−133.241 978
$CH_3^•$	−39.572 913	−39.707 171	−39.728 100	−39.730 6361

[a] Single-point calculations (hartree) on the 6-31G* optimized geometries. [b] I: single point calculations on optimized ion geometries. [c] N: single point calculations on optimized neutral geometries.

methane peak in the NR spectrum of **1** points to the formation of $C_2H_4N^+$ by stepwise elimination of CH_3 and H.

Collisional activation of neutral **1**, **1a**, and **1b** decreases the survivor ion relative intensities by 40, 70, and 52%, respectively (Table I). $[C_2H_4N]^+$ decreases by 15% upon neutral CAD whereas the ratios of $[C_2H_5N]^{•+}$,$[C_2H_4N]^+$ and their deuterated analogs do not change appreciably. This suggests that the mechanisms for the CH_3 and (CH_3 + H) eliminations do not change upon neutral excitation. The largest increase upon neutral CAD is observed for $[CH_3]^+$ and $[CD_3]^+$ from **1a** and **1b** (30–40%) and $[CN]^+$, $[HCN]^{•+}$, and $[H_2CN]^+$. The latter are mostly due to ion dissociations following reionization of the C_2H_5N intermediate formed by loss of methyl from **1**. Consistent with this, the NR mass spectra of three C_2H_5N isomers (Figure 2) show abundant ions at m/z 26–28.

Relative Energies and Dissociation Mechanisms. In order to interpret the spectral data, total (Tables III and IV) and relative energies (Table V) of the neutral and ionic species relevant to **1** and $\mathbf{1}^+$ have been estimated by ab initio calculations. The relative enthalpies at 298 K can be compared with the experimental heats of formation given in Table V. Vertical neutralization of $\mathbf{1}^+$ is accompanied by large Franck–Condon effects resulting in 76 kJ mol^{-1} energy deposition in the radical formed (MP4/6-311G**, Table V). This is due to the large differences in the ion and radical equilibrium geometries as also reported recently.[10] The 6-31G* optimized geometry of $\mathbf{1}^+$ shows a short N–CH_2 bond (1.26 Å) and planar nitrogen and methylene centers, while in **1** the N–CH_2 bond is long (1.393 Å) and the nitrogen and methylene carbon centers are pyramidized (38 and 32°, respectively). The excitation energy in neutralized **1** is close to the 72 kJ mol^{-1} dissociation threshold calculated for $CH_3N{=}CH_2$ and $CH_3^•$ at the MP4/6-311G** level of theory (Table V). This compares well with the 81 kJ mol^{-1} dissociation endothermicity based on the revised $\Delta H_f(CH_3N{=}CH_2)$[28] (Table V). Investigations with a series of UHF/6-31G* calculations show a continuously increasing potential energy upon stretching one of the N–CH_3 bonds in **1**. Simultaneously, the CH_2 group is flattened and rotates to become co-planar with the H_3C–N–C plane. As the CH_3–N bond is elongated (e.g., 2 Å in Figure 3) the spin density is delocalized from the methylene group in **1** to the nitrogen atom

(28) Peerboom, R. A. L.; Ingemann, S.; Nibbering, N. M. M.; Liebman, J. F. *J. Chem. Soc., Perkin Trans. 2* **1990**, 1825–1828.

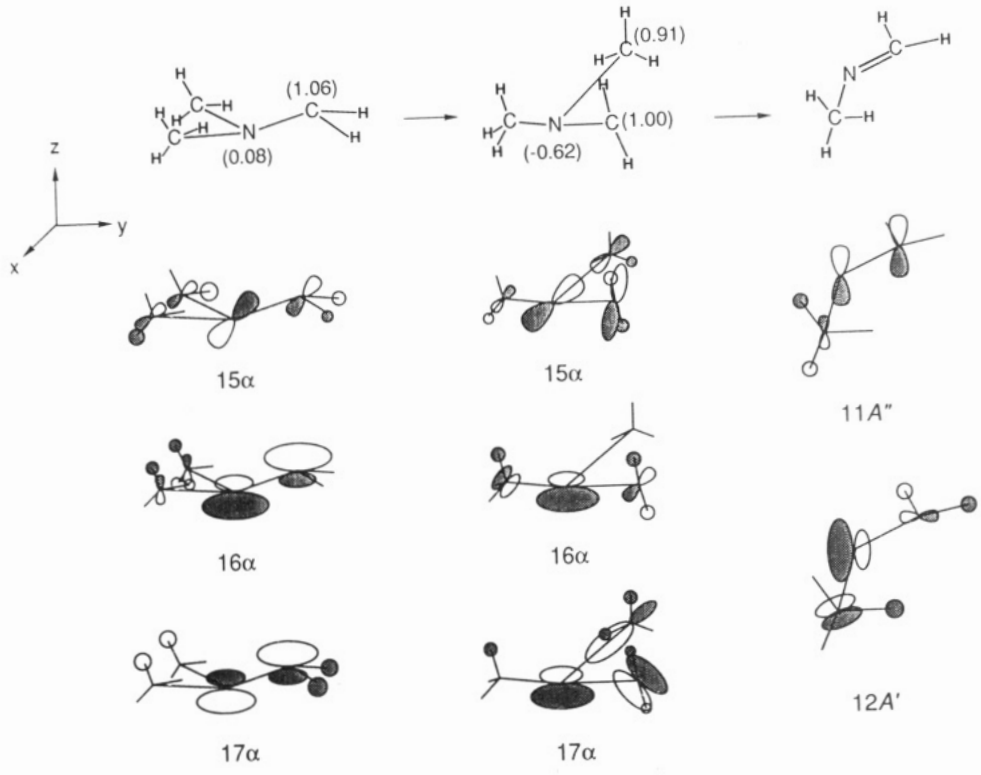

Figure 3. Orbital diagram for the loss of methyl from **1**. Atomic spin densities in parentheses.

Table V. Relative Energies[a]

species	MP4-(SDTQ)/6-31G*	MP2/6-311G**	MP4-(SDQ)/6-311G**	ΔH_f
neutrals				
1	0	0	0	109[b]
1 (I)[c]	81	74	76	
$CH_3N{=}CH_2 + CH_3$	69	80	72	190[b]
$\overline{CH_2CH_2NH} + CH_3$	112	123	123	272[b]
$(^1A_1)$**7** + CH_3	235			
$CH_2{=}NCH_2^{\bullet} + CH_4$	20			
$\overline{CH_2CH_2N}^{\bullet} + CH_4$	64			
$CH_3N{=}CH^{\bullet} + CH_4$	74			
ions				
$\mathbf{1}^+$	0 (469)[f]	0 (497)[f]	0 (503)[f]	649[d], 661[e]
$\mathbf{1}^+$ (N)[g]	87 (556)[f]	93 (590)[f]	95 (598)[f]	
$CH_3N{=}CH_2^{\bullet+} + CH_3$	447	469	430	1125[b]
$\overline{CH_2CH_2NH}^{\bullet+} + CH_3$	508	514	487	1160[b]
$(^2A_2)$**7**$^{\bullet+}$ + CH_3	378			
$CH_3N{\equiv}CH^+ + CH_4$	125			776[h]
$CH_2{=}N^+ = CH_2 + CH_4$	150			

[a] Relative enthalpies at 298 K, kJ mol^{-1}. [b] Reference 3. [c] From vertical neutralization of $\mathbf{1}^+$. [d] Reference 1. [e] Reference 9. [f] Relative to **1**. [g] From vertical ionization of **1**. [h] From the proton affinity of CH_3NC (ref 3) corrected according to ref 32.

and the departing methyl group. Orbital analysis shows that the SOMO (17α) in **1** correlates with the SOMO of the methyl radical. The HOMO (12a′) in $CH_3N{=}CH_2$ results from mixing of the 16α and 17α orbitals, whereas the π-orbital (11a″) develops from the 15α orbital in **1** through that in the intermediate structure (Figure 3).

Dissociations by loss of methyl to form the other stable C_2H_5N isomers with the C–N–C framework, e.g., aziridine and the $(^1A_1)$ $^{\bullet}CH_2NHCH_2^{\bullet}$ biradical (**7**),[29] are much more endothermic than that giving rise to $CH_3N{=}CH_2$ (Table V). In addition, the formations from **1** of aziridine and **7** require hydrogen migrations, so that methyl losses leading to these C_2H_5N isomers are likely to be kinetically disfavored against that forming $CH_3N{=}CH_2$.

(29) (a) Lien, M. H.; Hopkinson, A. C. *Can. J. Chem.* **1984**, *62*, 922–925. (b) Armstrong, D. R.; Walker, G. T. *J. Mol. Struct. (THEOCHEM)* **1987**, *149*, 369–389.

The thermochemical thresholds for methane eliminations from neutral **1** to give the 1-aziridinyl or (methylimino)methinyl radicals are comparable to the threshold for the methyl loss forming $CH_3N{=}CH_2$, while methane elimination forming the 2-azaallyl radical shows a much lower threshold (Table V). These thermochemical thresholds indicate that the dissociation energies of the N—H bond in aziridine and the N=CH—H bond in $CH_3N{=}CH_2$ are similar to the dissociation energy of the C—H bond in methane, whereas the $H{-}CH_2N{=}CH_2$ bond is 49 kJ mol^{-1} weaker. However, methane elimination that would form $CH_2{=}NCH_2^{\bullet}$ is not observed experimentally (vide supra) and should thus have a high activation barrier.

We have further examined computationally (UHF/6-31G*) the energy barriers in the reverse addition of methane to $CH_3N{=}CH^{\bullet}$; methane addition and elimination would presumably have identical transition states due to the principle of microscopic reversibility. However, a substantial increase of potential energy resulted when the methane molecule approached the nitrogen atonm in (*Z*)-$CH_3N{=}CH^{\bullet}$ at various $H_4C{-}N{=}C$ angles and $H_4C{-}H{=}C{-}H$ dihedral angles. For example, a planar configuration with a 2.0-Å H_4C–N distance is calculated to be 330 kJ mol^{-1} less stable than **1**, with a large negative energy gradient along the C–N bond, suggesting a further energy increase upon closer approach. Out-of-plane configurations at the same C–N distance show even higher potential energies. Although we did not locate the transition state, it follows from these calculations that there must be substantial barriers to concerted methane eliminations from neutral **1**. Hence, consistent with the previous pyrolytic experiments,[11] the loss of methyl from **1** appears to be the favored dissociation pathway; the apparent elimination of methane in the NR spectrum is therefore due to a combination of neutral and ion dissociations.

Vertical reionization of **1** is accompanied by large Franck–Condon effects resulting in a 95 kJ mol^{-1} energy excess in the $\mathbf{1}^+$ formed (Table V). The calculated ionization energies visibly increase with using the larger 6-311G** basis set, whereas including fourth-order Møller–Plesset corrections has only a small effect (Table V). Our best adiabatic ionization energy (5.21 eV) is somewhat lower than the experimental estimate from the

Scheme III

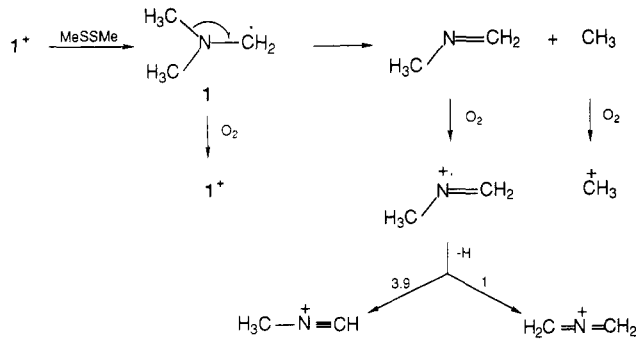

difference in the ion and neutral enthalpies of formation.[1,9] The corresponding neutral vertical ionization energy and ion recombination energy (calculated as 6.30 and 4.53 eV, respectively) have not been determined previously. Note that the latter value is lower than the ionization energy of sodium, justifying the description of **1** as an "organic alkali metal".[1b]

The calculations show low thermochemical thresholds for the eliminations of methane from $\mathbf{1}^+$ in good agreement with the experimental value for the formation of $CH_3N{\equiv}CH^+$ (Table V). By analogy with alkane eliminations from immonium ions,[6g] the methane eliminations from $\mathbf{1}^+$ probably involve activation barriers that affect the branching ratio for the formation of $CH_3N{\equiv}CH^+$ and $CH_2{=}N^+{=}CH_2$. Nevertheless, the formation of the more stable $CH_3N{\equiv}CH^+$ is consistent with the prevalent methane elimination from $\mathbf{1}^+$ involving transfer of a methylene hydrogen atom, as evidenced by the labeling data. Losses of methyl from $\mathbf{1}^+$ leading to $C_2H_5N^{•+}$ isomers are calculated to be much more endothermic again in good agreement with the experimental enthalpies (Table V).

The dissociations observed in the NR spectra of $\mathbf{1}^+$ can be explained by combinations of neutral and ion reactions (Scheme III). Following neutralization, **1** dissociates predominantly by loss of methyl to form $CH_3N{=}CH_2$ as the most stable neutral C_2H_5N isomer (Table V). However, a subsequent loss of H from neutral $CH_3N{=}CH_2$ should give the more stable $CH_2{=}NCH_2^•$, in contradiction with the labeling data. Following reionization, loss of H from $CH_3N{=}CH_2^{•+}$ to give $CH_3N{\equiv}CH^+$ is favored by 25 kJ mol^{-1} against the formation of $CH_2{=}N^+{=}CH_2$, so that the former predominates. The greater stability of $CH_3N{\equiv}CH^+$ points to the reversal of the order of bond dissociation energies in the $CH_3N{=}CH_2^{•+}$ cation radical compared with the neutral imine, with the allylic C–H bond in the ion being *stronger* than the vinylic C–H bond (Table V).

Reionization of surviving **1** may also induce fragmentation of the ion $\mathbf{1}^+$ formed. Note that Franck–Condon effects alone would not account for $\mathbf{1}^+$ dissociations due to the substantial stability of $\mathbf{1}^+$ (Table V). The NR spectrum of $\mathbf{1}^+$ shows only small peaks at m/z 57 and 30 which are typical for dissociations of $\mathbf{1}^+$. This and the different mechanism for $C_2H_4N^+$ formation suggest that dissociations of reionized $\mathbf{1}^+$ are less important than those of neutral **1**.

C_2H_5N Isomers. A peculiar feature of the NR spectrum of $\mathbf{1}^+$ is the low relative intensity of $CH_3N{=}CH_2^{•+}$, which represents a stable cation radical,[30] so the stability of this ion and its neutral counterpart was also of interest. The NR spectra of $CH_3N{=}CH_2^{•+}$ (from trimethylamine[31]), aziridine$^{•+}$, and its open-ring distonic isomer $^•CH_2NHCH_2^+$ ($\mathbf{7}^{•+}$ from dimethylamine[31]) differ in the relative abundances of the survivor ions at m/z 43 and those of fragments due to loss of hydrogen (m/z 42, Figure 2). Differences are also observed in the relative abundances of fragments at m/z 14 (N^+ and/or $CH_2^{•+}$), m/z 15 ($NH^{•+}$ and/or CH_3^+), and m/z 26–28; the latter also appear as common ion fragments in the CAD spectra of $C_2H_5N^+$ isomers.[31] The order of the survivor ion relative intensities, $[\mathbf{7}^{•+}] > [CH_3N{=}CH_2^{•+}] > [\text{aziridine}^{•+}]$, follows the order of *ion* not neutral stabilities (Tables III and V), suggesting that ion dissociations dominate. This is born out by the calculated reaction enthalpies (MP4/6-31G*) that show that dissociations of $CH_3N{=}CH_2^{•+}$ and $\mathbf{7}^{•+}$ by loss of H are less endothermic than those of their corresponding neutrals (eqs 1–4).

$$\mathbf{7}^{•+} \rightarrow CH_2{=}N^+{=}CH_2 + H^• \qquad \Delta H_{r,298} = 176 \text{ kJ mol}^{-1} \quad (1)$$

$$\mathbf{7} \rightarrow CH_2{=}NCH_2^• + H^• \qquad \Delta H_{r,298} = 189 \text{ kJ mol}^{-1} \quad (2)$$

$$CH_3N{=}CH_2^{•+} \rightarrow CH_3N^+{\equiv}CH + H^• \qquad \Delta H_{r,298} = 81.5 \text{ kJ mol}^{-1} \quad (3)$$

$$CH_3N{=}CH_2 \rightarrow CH_2{=}N\text{-}CH_2^• + H^• \qquad \Delta H_{r,298} = 355 \text{ kJ mol}^{-1} \quad (4)$$

The calculations also show very significant Franck–Condon effects in the neutralization and reionization of $CH_3N{=}CH_2$ and aziridine, but not singlet $^•CH_2NHCH_2^•$ (Tables III and IV). Vertical ionization of $CH_3N{=}CH_2$ deposits 67 kJ mol^{-1} in the ion formed, while neutralization of the ion forms the neutral with 105 kJ mol^{-1} internal energy (Table IV). These effects are almost entirely due to the different C–N–C angles in the ion (152.7°) and the neutral (118.6°) whereas the calculated neutral and ion C–H and C–N bond lengths are very similar.[29a] The energy deposition upon vertical transition between the ion and neutral potential energy surface will have a much greater effect on ion dissociations due to their lower endothermicities (eqs 1 and 3). This accounts for the low relative abundances of $CH_3N{=}CH_2^{•+}$ in its NR spectrum and in that of **1**, as reionization of the $CH_3N{=}CH_2$ neutral forms an excited ion which undergoes facile dissociation.

Similarly, vertical neutralization of aziridine$^{•+}$ deposits 70–72 kJ mol^{-1} in the neutral formed, whereas ionization leads to 53–56 kJ mol^{-1} excitation of the ion (Tables III and IV). Hence vertical reionization forms the aziridine ion with >10 kJ mol^{-1} excess energy above the thermochemical threshold for dissociation to $CH_2{=}N^+{=}CH_2$ and H$^•$, consistent with the negligible survivor ion relative intensity. The NR spectrum of aziridine also shows abundant $HCNH^+$, $HCN^{•+}$, CN^+, CH_3^+, and $CH_2^{•+}$, some of which are due to low-energy dissociations, e.g. the formation of CH_3^+ and $HCNH^+$ which requires 79 kJ mol^{-1}.[3]

Negligible Franck–Condon effects are expected for neutralization of the ground $^2A_2$ state $^+CH_2NHCH_2^•$ to form the ground $^1A_1$ state biradical **7** of a very similar equilibrium geometry (Figure 4). The NR spectrum of $\mathbf{7}^{•+}$ shows that biradical **7** is a thermodynamically stable, isolable species in line with ab initio calculations. The optimized triplet biradical (**8**) is calculated to be 122 kJ mol^{-1} less stable than **7** (Table III). Furthermore, formation of **8** by vertical neutralization of $\mathbf{7}^{•+}$ is expected to result in 57 kJ mol^{-1} energy deposition owing to the different geometries of the ion and the neutral formed, resulting in fast dissociation of the latter.

The calculated total energies for $CH_3N{=}CH_2$, aziridine, and their cation radicals allow us to evaluate the reliability of the computational methods used, by comparing the calculated vertical and adiabatic ionization energies with the experimental data from photoelectron spectra[11,30] ($CH_3N{=}CH_2$: IE_v = 9.90 eV, $IE_a \approx$ 9.4 eV; aziridine: IE_v = 9.85 eV, $IE_a \approx$ 9.2 eV).[3,23] MP4/6-31G* calculations (Table III) give $IE_v(CH_3N{=}CH_2)$ = 9.53

(30) Frost, D. C.; MacDonald, B.; McDowell, C. A.; Wrestwood, N. P. C. *J. Electron. Spectrosc. Relat. Phenom.* **1976**, *14*, 379–387.

(31) (a) Holmes, J. L.; Terlouw, J. K. *Can. J. Chem.* **1976**, *54*, 1007–1014. (b) Maquestiau, A.; Van Haverbeke, Y.; Flammang, R.; Menu, A. *Bull. Soc. Chim. Belg.* **1979**, *88*, 53–57.

(32) Meot-Ner (Mautner), M.; Sieck, L. W. *J. Am. Chem. Soc.* **1991**, *113*, 4448–4460.

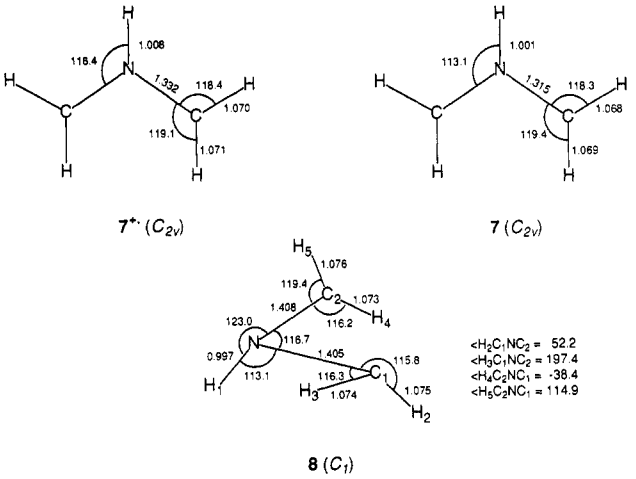

Figure 4. Calculated equilibrium geometries of ($^2A_2$) $\cdot CH_2NHCH_2^+$ ($7^{\cdot+}$), ($^1A_1$) $\cdot CH_2NHCH_2\cdot$ (**7**), and triplet $\cdot CH_2NHCH_2\cdot$ (**8**).

eV, $IE_a(CH_3N{=}CH_2)$ = 8.75 eV, IE_v(aziridine) = 9.37 eV, and IE_a(aziridine) = 8.78 eV. This shows that at this level of theory both the vertical and the adiabatic ionization energies are underestimated by 0.4–0.5 eV. Significant improvement is obtained for calculations using the 6-311G** basis set (Table IV). MP2/6-311G** calculations give ionization energies within 0.1–0.2 eV of the experimental values, e.g., IE_v = 9.99 and 9.74 eV and IE_a = 9.19 and 9.19 for $CH_3N{=}CH_2$ and aziridine, respectively. Inclusion of fourth-order excitations (MP4(SDQ)) results in a decrease in the calculated ionization energies, e.g. IE_v = 9.73 and 9.55 eV and IE_a = 8.92 and 8.98 eV for $CH_3N{=}CH_2$ and aziridine, respectively. These results indicate that calculations with the 6-311G** basis set of the vertical and adiabatic ionization energies of **1** produce reasonable estimates for this transient species, for which direct measurements are unavailable. Further improvement[33c] may be achieved in calculations that would include diffuse functions and multiple sets of *d* and *f* polarization functions as employed in the G2 theory.[33]

Conclusions

The experimental and theoretical data allow us to make the following conclusions. The (dimethylamino)methyl radical (**1**) is a stable species when formed by collisional neutralization of its cation. Loss of methyl to form *N*-methylmethylenimine is the dominant dissociation of neutral **1**, similar to its pyrolytic decomposition. Vertical neutralization forming **1** involves a large Franck–Condon effect, resulting in internal energy deposition. Similar effects are found by theory and experiment for collisional neutralization of the related C_2H_5N ions and for reionization of the corresponding neutral molecules. Theory and experiment are in accord in finding a stable $\cdot CH_2NHCH_2\cdot$ biradical which is predicted to be formed in its $^1A_1$ electronic state.

Acknowledgment. Support by the National Science Foundation (CHEM-9102442) and the donors of the Petroleum Research Fund, administered by the American Chemical Society, is gratefully acknowledged. Generous computer time allocation was provided by the Cornell National Supercomputer Facility that receives major funding from the National Science Foundation and the IBM corporation, with additional support from the New York State and the Corporate Research Institute.

Supplementary Material Available: Tables of 6-31G* optimized geometries and 6-31G* and 3-21G harmonic vibrational frequencies for the C_2H_5N, C_2H_4N, and C_3H_8N molecules and ions (7 pages). This material is contained in many libraries on microfiche, immediately follows this article in the microfilm version of the journal, and can be ordered from the ACS; see any current masthead page for ordering information.

(33) (a) Curtiss, L. A.; Raghavachari, K.; Trucks, G. W.; Pople, J. A. *J. Chem. Phys.* **1991**, *94*, 7221–7230. (b) Curtiss, L. A.; Raghavachari, K.; Pople, J. A. *J. Chem. Phys.* **1993**, *98*, 1283–1298. (c) Kuhns, D. W.; Tran, T. B.; Shaffer, S. A.; Turecek, F. *J. Am. Chem. Soc.* submitted for publication.